ЖЭТФ, 2002, том 121, вып. 6, стр. 1399–1414

SPECTRA OF REGULAR QUANTUM GRAPHS

Yu. Dabaghian**, *R. V. Jensen*, *R. Blümel

Department of Physics, Wesleyan University
Middletown, CT 06459-0155, USA

Submitted 18 December 2001

We consider a class of simple quasi one-dimensional classically nonintegrable systems that capture the essence of the periodic orbit structure of general hyperbolic nonintegrable dynamical systems. Their behavior is sufficiently simple to allow a detailed investigation of both classical and quantum regimes. Despite their classical chaoticity, these systems exhibit a «nonintegrable analogue» of the Einstein–Brillouin–Keller quantization formula that provides their spectra explicitly, state by state, by means of convergent periodic orbit expansions.

PACS: 05.45.Mt, 03.65.Sq, 02.30.Lt

1. INTRODUCTION

Very few quantum systems can be solved explicitly. Among them are the standard textbook examples, such as the harmonic oscillator or the hydrogen atom [1]. In all of these cases, the spectrum of the quantum system is obtained as an explicit analytical formula of the form «$E_n = \ldots$», where n is the quantum number of the system. This procedure already fails for some of the simplest quantum systems, which are still considered elementary textbook problems. An example is a quantum particle in a box with a step potential inside, as shown in Fig. 1. Even for the simple problem in Fig. 1, explicit analytical solutions of the form «$E_n = \ldots$» are no longer available because the problem leads to a transcendental spectral equation. The recommended method of solution is either numerical or graphical [1–3]. We recently found a way [4–6] of obtaining explicit analytical solutions of a wide class of problems such as the one shown in Fig. 1, thus obtaining an explicit analytical solution of textbook problems that until now were relegated to numerical or graphical solution techniques. Our methods are also a step forward in the mathematical theory of almost periodic functions [7], because we obtain explicit formulas for the zeros of a wide class of almost periodic functions. Furthermore, the classical dynamics of the quantum systems discussed in this paper is chaotic. Because it may well be true in general that the quantized versions of classically chaotic systems do not admit the existence

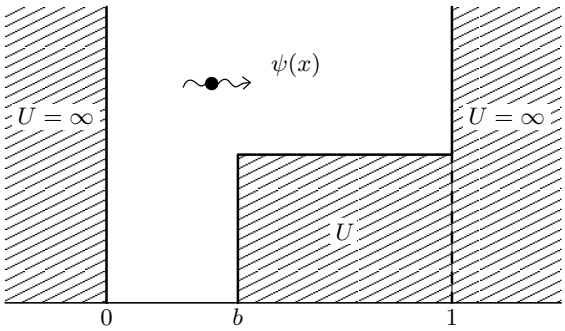

Fig. 1. Sketch of a step potential in a box, a well-known textbook quantum problem

of quantum numbers (see, e.g., [8, 9] for a detailed discussion of this important point), our «$E_n = \ldots$» spectral formulas, containing an explicit quantum number n, may come as a surprise. At this point, we feel that it is important to stress that our results are not conjectures, approximations or merely formal identities. Our results are exact, explicit, convergent periodic orbit expansions that can be cast into the form of mathematical theorems. We will publish the rigorous mathematical underpinnings of our results elsewhere [10].

It is well known [11] that the periodic orbit theory leads to completely different approaches for quantizing integrable and nonintegrable dynamical systems. For integrable systems, there is a simple procedure [11, 12] that allows quantizing the action variables individually for each degree of freedom. The situation is completely

*E-mail: ydabaghian@mail.wesleyan.edu

different for the chaotic case, where the periodic orbit theory [11] allows evaluating only certain global characteristics of the spectrum, e.g., the density of states

$$\rho(E) = \sum_{j=1}^{\infty} \delta\left(E - E_j\right) \approx \bar{\rho}(E) + \\ + \frac{1}{\pi} \operatorname{Im} \sum_{p} T_p(E) \sum_{\nu=1}^{\infty} A_p^{\nu}(E) \exp\left(i\nu S_p(E)\right), \quad (1.1)$$

typically with only semiclassical accuracy [13]. Here, $\bar{\rho}(E)$ is the average density of states, $S_p(E)$, $T_p(E)$, and $A_p(E)$ are respectively the action, the period, and the weight factor of the prime periodic orbit labeled by p, and ν is the repetition index. In this approach, individual energy levels are obtained indirectly as the singularities of the sum in Eq. (1.1). As for the idea of expressing them directly in terms of the periodic orbits, M. V. Berry wrote in 1991 [14]: « ... We do not know how, or even whether, the closed orbit sum generates the individual δs in the level density for chaotic systems. This is a serious – perhaps shocking – situation, because it means that we are ignorant of the mechanism of quantization.»

In the case of quantum graphs, Berry's question can be answered definitely. The periodic orbit sums representing the spectral density of quantum graphs do provide the individual levels in the form of δ-spikes in (1.1) and only those [15, 16, 17, 18]. In addition, we recently showed [4, 5, 6] that the answer to Berry's question can be taken one step forward: not only do periodic orbit expansions for quantum graphs produce δ-functions for the quantum states in the level density, but for certain classes of quantum graphs there also exist explicit convergent periodic orbit expansions for individual energy levels. Because they provide explicit formulas for the energy levels of classically chaotic systems, these periodic orbit expansions may be considered as «non-integrable analogues» of the Einstein–Brillouin–Keller (EBK) quantization formula [11, 12] that applies to integrable systems.

This paper is organized as follows. In Sec. 2, we briefly review the theory of quantum graphs and extend the theory by defining «dressed graphs», i.e., quantum graphs with arbitrary potentials on their bonds. In Sec. 3, we define an important class of dressed quantum graphs: regular quantum graphs. Based on a detailed study of their spectral properties in Sec. 3, we derive explicit analytical spectral formulas for regular quantum graphs in Sec. 4. In Sec. 5, we present a variety of regular quantum graphs illustrating the use and convergence of the spectral formulas. In Sec. 6, we summarize our results and conclude the paper.

2. DYNAMICAL NETWORKS

We consider a particle moving on a quasi one-dimensional network of bonds and vertices. These networks are known as graphs in the mathematical literature. They were and still are the subject of intensive investigations in all areas of science ranging from mathematics over computer science to chemistry and physics. An example of a simple graph with five vertices and seven bonds is shown in Fig. 2. The particle scatters randomly at every vertex V_i along different bonds B_{ij} that meet at that vertex. We assume that the graph contains a finite number of bonds and vertices (N_B and N_V respectively). The key assumption about the dynamics of the particle is that the turning points of any particle trajectory on the graph coincide with the vertices of the graph, and the shape of the trajectories is therefore uniquely determined by the geometry of the graph. The trajectories of the particle are simply the joint sequences of graph bonds, which are easily described and enumerated. For instance, every trajectory can be represented by a sequence of N_B symbols, each of which corresponds to a certain bond [19]. Because the trajectories correspond to various bond sequences, every trajectory is described by a code word consisting of N_B symbols.

We «dress» the bonds B_{ij} of the graph with potentials $U_{ij}(x)$, which may affect the way a particle moves along the bonds. However, it is required that these dressings do not violate the geometry of the particle trajectories, i.e., do not add turning points other than the original vertices of the graph. This condition is required to hold at all energies. To comply with this

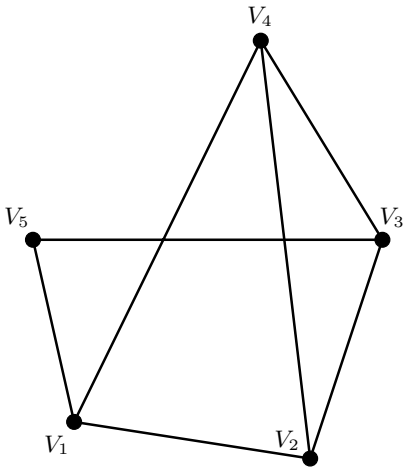

Fig. 2. Sample graph with five vertices and seven bonds

requirement, the bond potentials are allowed to depend on the energy E of the particle, i.e., $U_{ij} = U_{ij}(x, E)$, such that $E > U_{ij}(x, E)$ is fulfilled for all E and all i, j. This in fact leads to many additional simplifications that have a deep physical meaning in the context of the semiclassical periodic orbit theory [4–6, 19–21].

The shapes of the trajectories, and in particular of the periodic orbits, become increasingly complicated as their lengths grow. This makes them similar to the generic (dynamical) chaotic systems. In fact, the number of possible periodic orbits increases exponentially with their lengths, (or, equivalently, the number of vertex scatterings) with a rate which depends only on the topology of the graph. Every graph Γ can be characterized by its topological entropy (the global average rate of the exponential proliferation of periodic orbits)

$$\Lambda_\Gamma = \lim_{l\to\infty} \frac{\ln[\#(l)]}{l}, \tag{2.1}$$

where l characterizes the lengths of the periodic orbits in terms of the lengths of their code words and $\#(l)$ is the total number of periodic orbits of the length $\le l$ [9]. Because the phase space of the system is bounded, the dynamics of the particle is mixing [16], and hence, the structure of the periodic orbit set on dynamical networks closely imitates the behavior of the closed trajectories of generic chaotic systems [22, 23]. On the other hand, dynamical networks can be easily quantized [4–6, 17–19, 24], which makes them very convenient models for studying various aspects of quantum chaology.

The details of the classical dynamics on graphs are discussed in numerous publications [16, 25]. Below, we investigate the quantum-mechanical description of these systems. In particular, we discuss their spectra in the context of the periodic orbit theory. We now briefly outline some details of the graph quantization procedure that are used in the subsequent discussion.

A quantum graph system is a quantum particle that moves on a one-dimensional network Γ dressed with the potentials $U_{ij}(x, E)$. Below, we consider the case of scaling potentials discussed in [6, 26–28],

$$U_{ij}(E) = \lambda_{ij} E, \quad \lambda_{ij} = \lambda_{ji}, \tag{2.2}$$

where λ_{ij} are constants. This choice of the dressing potentials allows us to avoid certain mathematical complications, which are irrelevant for the physical context of our discussion. For more details on scaling potentials and their relevance to the semiclassical periodic orbit analysis, see [4, 6, 19].

The Schrödinger equation for graphs with potentials (2.2) can be written as

$$\hat{\pi}_{ij}^2 \psi_{ij}(x) = \beta_{ij}^2 E \psi_{ij}(x), \tag{2.3}$$

where

$$\hat{\pi}_{ij} = -i\frac{d}{dx} - A_{ij} \tag{2.4}$$

is the generalized momentum operator and

$$\beta_{ij}^2 = 1 - \lambda_{ij}.$$

The coordinate $0 \le x \le L_{ij}$ is measured along B_{ij} from i to j and $L_{ij} = L_{ji}$ is the length of the bond. The magnetic field vector potential $A_{ij} = -A_{ji}$ is assumed to be a constant real matrix; it can be used as a tool for breaking the time-reversal symmetry.

Classically, the particle can travel along the bond B_{ij} if its energy is above the scaled potential height, $E > U_{ij}(E)$ $(\lambda_{ij} < 1)$. In this case, the solution of Eq. (2.3) on the bond B_{ij} is a combination of free waves,

$$\psi_{ij}(x) = a_{ij}\frac{\exp\left(i\left(-\beta_{ij}k + A_{ij}\right)x\right)}{\sqrt{\beta_{ij}k}} + b_{ij}\frac{\exp\left(i\left(\beta_{ij}k + A_{ij}\right)x\right)}{\sqrt{\beta_{ij}k}}, \tag{2.5}$$

where $k = \sqrt{E}$ and the factors $(\beta_{ij}k)^{-1/2}$ are introduced to separate the physically meaningful flux amplitudes from the coefficients a_{ij} and b_{ij}. In the opposite case where $\lambda_{ij} > 1$, the bond B_{ij} carries a linear combination of tunneling solutions. Due to the scaling assumption, there is no transition between these two cases as a function of E. From now on, we assume that the energy E is kept above the maximum scaled potential height,

$$\lambda_{ij} < 1, \quad i, j = 1, \ldots, N_V. \tag{2.6}$$

At every vertex V_i, the bond wave functions satisfy the boundary conditions

$$\begin{aligned} &\psi_{ij}(x=0) = \varphi_i C_{ij}, \\ &\sum_{j=1}^{N_V} C_{ij}\hat{\pi}_{ij}\psi_{ij}(x)|_{x=0} = -i\lambda_i\varphi_i \end{aligned} \tag{2.7}$$

for all $i, j = 1, \ldots, N_V$. Here, C_{ij} is the connectivity matrix of the graph, φ_i is the value of the wave function at the vertex V_i, and λ_i are free parameters of the problem, scaled as $\lambda_i = \lambda_i^0 k$ (see the Appendix). We note that the double-indexed scaling constants λ_{ij} refer to the bonds, whereas the single-indexed constants

λ_i refer to the scattering strengths at the vertices. We believe that this notation is natural and does not lead to confusion.

Conditions (2.7) are consistent only for a discrete set of energy levels $E_n = k_n^2$ that define the spectrum of the dressed quantum graph problem (2.3) and (2.7). As shown in [6, 16–18, 24] (see the Appendix), using the scattering quantization approach [29] allows one to obtain the spectral equation for any quantum graph problem in the form

$$\Delta(k) = \det[1 - S(k)] = 0, \tag{2.8}$$

where $S(k)$ is the finite unitary graph scattering matrix [16]. The indices that define the matrix elements S_{IJ} of the matrix S correspond to the graph bonds. It is important that the bond $B_I \equiv B_{ij}$ is considered to be different from the (geometrically identical) reversed bond $B_{I'} \equiv B_{ji}$; the bonds of the graph are therefore directed [4–6, 16, 18]. Hence, the dimensionality of the scattering matrix is $2N_B \times 2N_B$. It is shown in the Appendix that $S = TD(k)$, where T is a constant $2N_B \times 2N_B$ unitary matrix and D is the diagonal unitary matrix with the matrix elements

$$\begin{aligned} D_{IJ} &= \delta_{IJ} \exp\left(i\left(\beta_I k + A_I\right) L_I\right), \\ I &= 1, \ldots, 2N_B. \end{aligned} \tag{2.9}$$

Because $\Delta(k)$ is a complex function, it is convenient to define the spectrum via the zeros of its absolute value,

$$|\Delta(k)| = \exp\left(-i\Theta_0(k)\right)\Delta(k), \tag{2.10}$$

where $\Theta_0(k)$ is the complex phase of $\Delta(k)$. The logarithmic derivative of $|\Delta(k)|$ produces a delta-peak for each of its roots,

$$-\frac{1}{\pi}\,\mathrm{Im}\lim_{\epsilon\to 0}\frac{d}{dk}\ln|\det\left[1 - S\left(k + i\epsilon\right)\right]| = \sum_{n=1}^{\infty}\delta(k - k_n), \tag{2.11}$$

which, by definition, is the density of the momentum states $\rho(k)$ [6]. On the other hand, using (2.10) and expanding the logarithm of determinant (2.8), the density of states can be written as

$$\rho(k) = \frac{1}{\pi}\frac{d\Theta_0(k)}{dk} + \frac{1}{\pi}\,\mathrm{Im}\frac{d}{dk}\sum_{n=1}^{\infty}\frac{1}{n}\,\mathrm{Tr}\left[S(k)\right]^n. \tag{2.12}$$

It can then be easily seen from the structure of the scattering matrix S [16, 24] that the matrix elements of its n-th power are defined on connected sequences of n bonds and the trace of S^n generates terms defined on closed connected sequences of n bonds [6, 17, 24, 25].

These periodic connected sequences of n bonds B_{ij} can be viewed as the periodic orbits traced by a classical point particle moving on the graph. We note that the phase of the exponential in (2.9) is exactly the action of a classical point particle trajectory traversing the bond B_I,

$$\mathcal{S}_I = \int_{B_I}\left(\beta_I k + A_I\right)dx = \left(\beta_I k + A_I\right)L_I. \tag{2.13}$$

Therefore, the semiclassical transition amplitudes $\exp(i\mathcal{S}_I)$ between the vertices connected by the bond B_I determine the scattering matrix $S(k)$. As a consequence [4–6, 16, 19], the «closed bond sequence expansion» (2.12) can be explicitly written as a periodic orbit expansion in terms of phases (2.13),

$$\rho(k) = \bar{\rho}(k) + \frac{1}{\pi}\,\mathrm{Re}\sum_p S_p^0\sum_{\nu=1}^{\infty}A_p^\nu\exp(i\nu S_p^0 k), \tag{2.14}$$

where S_p^0 is the k-independent «action length» of the orbit p,

$$S_p = \sum_p \beta_{ij}L_{ij}k \equiv S_p^0\,k, \tag{2.15}$$

and A_p is its weight containing the constant factor $\exp(i\sum_p A_{ij}L_{ij})$. Because of the scaling assumption (see the Appendix), the weight factor A_p is k-independent. The first term in this expression corresponds to the average density of states of the momentum $\bar{\rho}(k)$,

$$\bar{\rho}(k) = \frac{1}{\pi}\frac{d\Theta_0(k)}{dk}, \tag{2.16}$$

while the periodic orbit sum in (2.14) describes the fluctuations around the average.

The periodic orbit expansion for the staircase function

$$N(k) = \sum_{n=1}^{\infty}\Theta(k - k_n) \tag{2.17}$$

can be obtained by direct integration of (2.11) and (2.14). We obtain

$$N(k) = \bar{N}(k) + \tilde{N}(k), \tag{2.18}$$

where the first term

$$\bar{N}(k) = \int_0^k \bar{\rho}(k')\,dk' + \bar{N}(0) \tag{2.19}$$

represents the average behavior of the staircase and

$$\tilde{N}(k) = \mathrm{Im}\,\frac{1}{\pi}\sum_p\sum_{\nu=1}^{\infty}\frac{A_p^\nu}{\nu}\exp(i\nu S_p^0 k) \tag{2.20}$$

describes zero-mean oscillations around the average.

As discussed in the Introduction (see also [4–6, 16, 25]), quantum graphs are chaotic in the classical limit. The classical scattering probabilities are obtained in the limit as $\hbar \to 0$ from the quantum mechanical transition amplitudes [4–6] (see the Appendix). In the scaling case, they are k-independent, and therefore, the quantum scattering amplitudes do not depend on $\hbar$ at all. They determine the quantum and the classical scattering probabilities simultaneously.

3. REGULAR GRAPHS AND THEIR SPECTRA

The spectral determinant is a polynomial of degree $2N_B$ of the matrix elements of S. It was shown in [6] that the total phase of this polynomial is

$$\Theta_0(k) = \frac{1}{2}\,\mathrm{Im}\ln\det S(k) = kS_0 - \pi\gamma_0, \tag{3.1}$$

where

$$S_0 = \sum_{(ij)} L_{ij}\beta_{ij}$$

is the total action length of the graph Γ and

$$\gamma_0 = \frac{N_B + N_V}{2} + \frac{1}{\pi}\sum_{i=1}^{N_V} \mathrm{arctg}\left(\frac{\lambda_i^0}{v_i}\right), \tag{3.2}$$

where

$$v_i = \sum_j C_{ij}\,\beta_{ij}. \tag{3.3}$$

The average density of states is therefore a constant,

$$\bar{\rho} = \frac{1}{\pi}\frac{d}{dk}\Theta_0(k) = \frac{S_0}{\pi}, \tag{3.4}$$

and the average staircase function in Eq. (2.19) is

$$\bar{N}(k) = \frac{S_0}{\pi}k + \bar{N}(0). \tag{3.5}$$

The spectral equation $|\Delta(k)| = 0$ can be written as

$$\cos\left(S_0k - \pi\gamma_0\right) = \sum_{i=1}^{N_\Gamma} a_i\cos(S_ik - \pi\gamma_i), \tag{3.6}$$

where the frequencies $S_i < S_0$ are combinations of the reduced classical actions $S_{ij}^0 = \beta_{ij}L_{ij}$, and γ_0, γ_i are constants. The number N_Γ of terms in (3.6) is bounded by $N_\Gamma \le 3^{N_B}$ [6].

The frequency S_0 in $\Theta_0(k)$ is the largest frequency in expansion (3.6). While it is the only characteristic of the graph contained in the left-hand side of (3.6), the right-hand side

$$\Phi(k) \equiv \sum_{i=1}^{N_\Gamma} a_i\cos(S_ik - \pi\gamma_i), \tag{3.7}$$

contains the complete information about the graph system. We call $\Phi(k)$ the characteristic function of the graph.

A graph Γ is called regular [4–6] if its characteristic function $\Phi(k)$ satisfies

$$\sum_{i=1}^{N_\Gamma} |a_i| \equiv \alpha < 1. \tag{3.8}$$

For regular graphs, spectral equation (3.6) can be solved formally [4–6] to yield the implicit equation of its eigenvalues,

$$k_n = \frac{\pi}{S_0}\left[n + \mu + \gamma_0\right] + \frac{1}{S_0}\times \\ \times\begin{cases} \arccos[\Phi(k_n)] & \text{for} \quad n+\mu \quad \text{even}, \\ \pi - \arccos[\Phi(k_n)] & \text{for} \quad n+\mu \quad \text{odd}, \end{cases} \tag{3.9}$$

where μ is a fixed integer, chosen such that k_1 is the first positive solution of (3.6). The index $n \in \mathbb{N}$ labels the roots of (3.6) in their natural order.

The implicit form in Eq. (3.9) immediately implies that because the second term in (3.9) is bounded by π/S_0, the deviations of solutions to this equation from the points

$$\hat{k}_n = \frac{\pi}{S_0}(n + \mu + \gamma_0 + 1) \tag{3.10}$$

never exceed π/S_0 in absolute value for any n. The quantities $\hat{k}_n$ are very important in what follows because they determine the root structure of (3.6).

The roots k_n can be decomposed into an average part $\bar{k}_n$ and a fluctuating part $\tilde{k}_n$. From (3.9), we obtain

$$k_n = \bar{k}_n + \tilde{k}_n, \tag{3.11}$$

where

$$\bar{k}_n = \frac{\pi}{S_0}\left[n + \mu + \gamma_0 + \frac{1}{2}\right], \tag{3.12}$$

and

$$\tilde{k}_n = \frac{(-1)^{n+\mu}}{S_0}\left\{\arccos[\Phi(k_n)] - \frac{\pi}{2}\right\}. \tag{3.13}$$

We note that the constant $\mu+\gamma_0$ can be related to the initial value $\bar{N}(0)$ of the average staircase function in Eq. (3.5). We now consider the integral

$$\lim_{n\to\infty}\frac{1}{\hat{k}_n}\int_0^{\hat{k}_n} N(k')dk'. \tag{3.14}$$

The integration in (3.14) can be easily performed because the function $N(k)$ has simple form (2.17),

$$\frac{1}{\hat{k}_n}\int_0^{\hat{k}_n} N(k')dk' = n - \frac{1}{\hat{k}_n}\sum_{i=1}^{n} k_i, \tag{3.15}$$

since there are n roots to the left of $\hat{k}_n$. The fluctuations of both $N(k)$ and k_n around their average values have zero mean, and in the limit of $n \gg 1$ we can therefore use $\bar{N}(k)$ and $\bar{k}_n$ instead of $N(k)$ and k_n in (3.15) and write

$$\frac{1}{\hat{k}_n}\int_0^{\hat{k}_n} \bar{N}(k')dk' = n - \frac{1}{\hat{k}_n}\sum_{i=1}^{n} \bar{k}_i, \quad n \gg 1. \tag{3.16}$$

Using the explicit forms of $\hat{k}_n$, $\bar{k}_n$, and $\bar{N}(k)$, we obtain

$$\bar{N}(0) + \frac{1}{2}(n+\mu+\gamma_0+1) = \\ = \frac{n}{n+\mu+\gamma_0+1}\left(\frac{n}{2}+\mu+\gamma_0+1\right). \tag{3.17}$$

Expanding the right-hand side and keeping terms up to the order $1/n$ yields

$$\bar{N}(0) + \frac{1}{2}(n+\mu+\gamma_0+1) = \\ = n - \left(1 - \frac{\mu+\gamma_0+1}{n}\right)\left(\frac{n}{2}+\mu+\gamma_0+1\right). \tag{3.18}$$

The terms proportional to n cancel. Comparing the constants in (3.18) yields

$$\bar{N}(0) = -(\mu+\gamma_0+1). \tag{3.19}$$

It can be verified by direct substitution that

$$\bar{N}(\hat{k}_n) = n, \tag{3.20}$$

which implies that function (3.10) is the inverse of average staircase function (3.5). The points $\hat{k}_n$ can also be viewed as the intersection points of staircase function (2.17) and its average (3.5),

$$\bar{N}(\hat{k}_n) = N(\hat{k}_n) = n, \tag{3.21}$$

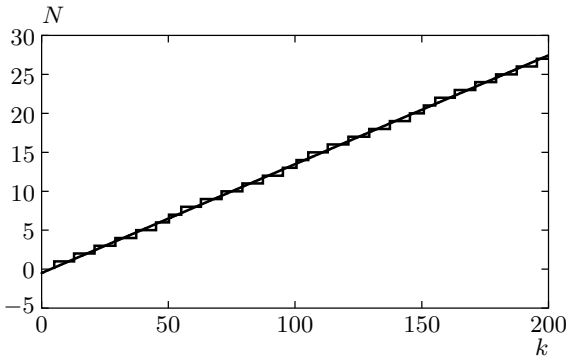

Fig. 3. The exact spectral staircase function $N(k)$ and its average $\bar{N}(k)$ for the scaling step potential shown in Fig. 1 with $b = 0.3$ and $\lambda = 1/2$. The average $\bar{N}(k)$ crosses every «stair» of $N(k)$ (piercing average) at the equally spaced separating points $\hat{k}_n$

and hence, the fluctuations $\tilde{N}(k)$ of the spectral staircase vanish at the points $\hat{k}_n$,

$$\tilde{N}(\hat{k}_n) = \mathrm{Im}\,\frac{1}{\pi}\sum_p\sum_{\nu=1}^{\infty}\frac{A_p^\nu}{\nu}\exp(i\nu S_p^0\hat{k}_n) = 0. \tag{3.22}$$

Geometrically, Eq. (3.22) means that the average staircase function $\bar{N}(k)$ intersects every step of the staircase function $N(k)$. We therefore call $\bar{N}(k)$ the piercing average. This is illustrated in Fig. 3, which shows the spectral staircase function $N(k)$ for the scaling step potential shown in Fig. 1 and discussed in more detail in Sec. 5, Example 1, below. We used the parameters $\lambda = 1/2$ and $b = 0.3$. Also shown is the average staircase $\bar{N}(k)$ for this case. It clearly pierces all the steps of $N(k)$, providing an example of a system with a piercing average.

Because $\Phi(k)$ contains only frequencies smaller than S_0, every open interval $I_n = (\hat{k}_{n-1}, \hat{k}_n)$ contains only one root of (3.6), namely k_n, and therefore, $\hat{k}_n$ play the role of separating points between adjacent roots [4–6, 10]. Moreover, because of (3.8), the «allowed zones» $R_n \subset I_n$ where the roots k_n can be found narrow to

$$k_n \in R_n \equiv \left(\frac{\pi}{S_0}(n+\mu+\gamma_0+u), \right. \\ \left. \frac{\pi}{S_0}(n+\mu+\gamma_0+1-u)\right), \tag{3.23}$$

where $u = \arccos\alpha/S_0$. Correspondingly, there are for-

bidden regions F_n,

$$F_n \equiv \left(\frac{\pi}{S_0}\,(n+\mu+\gamma_0-u)\,, \right. \\ \left. \frac{\pi}{S_0}\,(n+\mu+\gamma_0+1+u) \right) \qquad (3.24)$$

where roots of (3.6) never appear. In the limit as $\alpha \to 1$ ($u \to 0$), the allowed zones R_n tend to occupy the entire root interval, $R_n \to I_n$.

4. SPECTRAL FORMULAS

Once the existence of separating points $\hat{k}_n$ has been established, it is possible to obtain an exact periodic orbit expansion separately for every root of (2.8). The derivation is based on the identity

$$k_n = \int\limits_{\hat{k}_{n-1}}^{\hat{k}_n} k\rho(k)dk. \qquad (4.1)$$

Substituting exact periodic orbit expansion (2.14) for $\rho(k)$ in (4.1) yields

$$k_n = \int\limits_{\hat{k}_{n-1}}^{\hat{k}_n} k\frac{S_0}{\pi}dk + \\ + \frac{1}{\pi}\int\limits_{\hat{k}_{n-1}}^{\hat{k}_n} k\,\mathrm{Re}\sum_p S_p^0 \sum_{\nu=1}^{\infty} A_p^\nu \exp(i\nu S_p^0 k)dk = \\ = \frac{\pi}{S_0}\left(n+\mu+\gamma_0+\frac{1}{2}\right) + \\ + \hat{k}_n\,\mathrm{Im}\,\frac{1}{\pi}\sum_p\sum_{\nu=1}^{\infty}\frac{A_p^\nu}{\nu}\exp(i\nu S_p^0\hat{k}_n) - \\ - \hat{k}_{n-1}\,\mathrm{Im}\,\frac{1}{\pi}\sum_p\sum_{\nu=1}^{\infty}\frac{A_p^\nu}{\nu}\exp(i\nu S_p^0\hat{k}_{n-1}) + \\ + \mathrm{Re}\,\frac{1}{\pi}\sum_p\frac{1}{S_p^0}\times \\ \times\sum_{\nu=1}^{\infty}\frac{A_p^\nu}{\nu^2}\left(\exp(i\nu S_p^0\hat{k}_n)-\exp(i\nu S_p^0\hat{k}_{n-1})\right). \qquad (4.2)$$

Using (3.22), we simplify (4.2) to

$$k_n = \frac{\pi}{S_0}\left(n+\mu+\gamma_0+\frac{1}{2}\right) - \\ - \frac{1}{\pi}\,\mathrm{Im}\sum_p\frac{2}{S_p^0}\sum_{\nu=1}^{\infty}\frac{A_p^\nu}{\nu^2}\sin\left[\frac{\nu\omega_p}{2}\right]\times \\ \times\exp\left[i\nu\omega_p\left(n+\mu+\gamma_0+\frac{1}{2}\right)\right], \qquad (4.3)$$

where $\omega_p = \pi S_p^0/S_0$. The series expansion for k_n in Eq. (4.3) is more than a formal identity. It is rigorously convergent, however it converges only conditionally, which means that the result of the summation depends on how the summation is performed. Indeed, according to the well-known Riemann reordering theorem, one can obtain any result by rearranging the terms of a conditionally convergent series [30]. For the proper convergence of (4.3) to the exact roots of spectral equation (3.6), we must therefore specify how the terms in (4.3) are to be summed.

The mathematical details of the convergence properties of (4.3) are presented in [10]. We here mention the main result, which states that the terms in (4.3) must be summed according to the length of the symbolic codes [6, 19] of the periodic orbits, and not according to their action lengths. If (4.3) is summed in this way, it not only converges, but also converges to the exact roots k_n of spectral equation (3.6).

Equation (4.3) therefore provides an explicit representation of the roots of spectral equation (2.8) in terms of the geometric characteristics of the graph. In accordance with (3.12), the first term in (4.3) is the average value $\bar{k}_n$ and the following periodic orbit sum is an explicit expression for the fluctuation of the root $\tilde{k}_n$. This method is not limited to obtaining explicit analytical periodic orbit expansions for k_n. In fact, using the identity

$$f(k_n) = \int\limits_{\hat{k}_{n-1}}^{\hat{k}_n} f(k)\rho(k)dk, \qquad (4.4)$$

we can obtain periodic orbit expansions for any function of the eigenvalues $f(k_n)$, for instance for the energy $E = k^2$.

In the simplest case where $\lambda_i^0 = 0$, $A_{ij} = 0$, and $\mathrm{Im}\,A_p = 0$, we have

$$k_n = \frac{\pi}{S_0}n - \\ - \frac{2}{\pi}\sum_p\frac{1}{S_p^0}\sum_{\nu=1}^{\infty}\frac{A_p^\nu}{\nu^2}\sin\left(\frac{1}{2}\nu\omega_p\right)\sin(\nu\omega_p n). \qquad (4.5)$$

We note that $k_{-n} = -k_n$ in this case.

Both the EBK theory and formula (4.3) allow us to compute energy eigenvalues explicitly. In this sense, formula (4.3) may be regarded as an analogue of the EBK quantization formula [11, 12] for a chaotic system. The complexity of this expansion, structurally similar to (1.1), reflects the geometrical complexity of the periodic orbit set for graph systems.

Finally, for explicit calculations (see Sec. 5), it remains to determine the explicit form of the expansion coefficients A_p. For some simple graphs, this was done in [16, 19]. In the Appendix, we solve the problem for general dressed graphs. We show that every passage of an orbit p from a bond B_{ij} to $B_{ij'}$ through a vertex V_i contributes a factor $\sigma_{ji,ij'}$ (a matrix element of the matrix T, see the Appendix) to the weight A_p of the orbit,

$$A_p = \prod \sigma^{(i)}_{jj'}, \tag{4.6}$$

where the product is taken over the sequence of the bonds traced by the orbit p.

5. EXAMPLES

In (3.8), we provided the definition of regular quantum graphs; in (3.9)–(3.24), we then discussed analytical properties of their spectra. The discussion of regular quantum graphs culminated in Sec. 4 with the derivation of explicit spectral formulas for individual quantum states of regular quantum graphs. However, the above definition of regular quantum graphs does not imply that regular quantum graphs actually exist. Examples 1–3, discussed below, provide specific instances of quantum graphs that are regular for all choices of their parameters. Examples 4 and 5 present quantum graphs that exhibit both regular and irregular regimes. Finally, examples 6 and 7 provide illustrations of a new class of quantum graphs, marginal quantum graphs, for which

$$\sum_{i=1}^{N_\Gamma} |a_i| = 1.$$

Except for special choices of their dressing potentials, these graphs can still be accommodated within the mathematical framework set up in Secs. 3 and 4 and also admit an explicit representation of their spectra in accordance with the spectral formulas derived in Sec. 4.

Example 1: Scaling step potential in a box. We consider a particle confined to a box $0 < x < 1$ containing the scaling step potential (see Figs. 1 and 4*a*)

$$U(x) = \begin{cases} 0 & \text{for} \quad 0 < x \le b, \\ \lambda_{23} E & \text{for} \quad b < x < 1. \end{cases} \tag{5.1}$$

This is equivalent to a three-vertex linear chain graph (Fig. 4*a*′) with $\lambda_2 = 0$, $A_{ij} = 0$, and the Dirichlet boundary conditions at V_1 and V_3. This example is also discussed in [4, 5, 6, 19, 31]. In this case, spectral equation (3.6) can be written as [4, 5]

$$\sin\left[k(S^0_{21} + S^0_{23})\right] = r \sin\left[k(S^0_{21} - S^0_{23})\right], \tag{5.2}$$

where

$$r = \frac{1 - \beta_{23}}{1 + \beta_{23}} < 1 \tag{5.3}$$

is the reflection coefficient at the vertex V_2. Regularity condition (3.8) is therefore automatically satisfied and this graph is always regular. In Sec. 4, we already discussed the convergence properties of (4.3), including the fact that a rigorous mathematical proof for the convergence of (4.3) exists [10]. Here, we present solid numerical evidence for the convergence of (4.3) in the context of scaling step potential (5.1). As discussed in [4, 5, 6, 19], every periodic orbit in potential (5.1) can be described by a binary code word. Figure 5 shows the relative error

$$\epsilon^{(l)}_n = \frac{|k^{(l)}_n - k_n|}{k_n}, \quad n = 1, 10, 100$$

of the result $k^{(l)}_n$ predicted by (4.3) compared to the numerically obtained exact result k_n as a function of the binary code length l of the orbits used in expansion (4.3). We used $b = 0.3$ and $\lambda = 1/2$. Figure 5 also demonstrates that using all periodic orbits up to the binary code length $l \sim 150$, we obtain an accuracy on the order 10^{-4}–10^{-7} for the roots k_n of (5.2). Although the convergence of the series is slow (according to Fig. 5, it is approximately of the order $1/l^2$ on average), one can obtain a sufficiently good estimate for the roots using all orbits of the code length 20 and smaller.

Example 2: Scaling δ function in a box. This potential, shown in Fig. 4*b*, is again equivalent to a three-vertex quantum graph. This time, however, the potentials on the bonds are identically zero, whereas the vertex V_2 is dressed with a scaling δ function of strength

$$\lambda_2 = \lambda^0_2 k > 0.$$

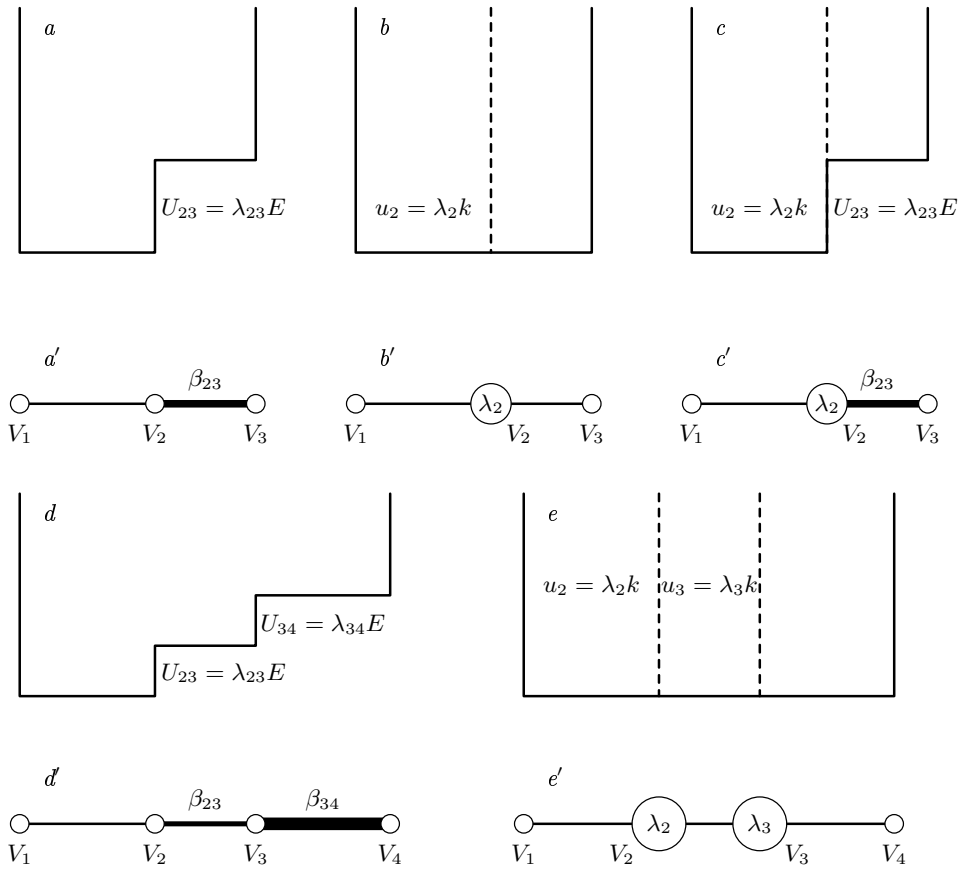

Fig. 4. Collection of potentials and their associated linear quantum graphs that serve as examples to illustrate the concept of regular quantum graphs. a — Scaling step potential in a box and its associated three-vertex linear graph (a'). b — Scaling δ function in a box and its corresponding three-vertex linear graph (b'). Combined scaling δ function and step potential in a box (c) with its linear three-vertex quantum graph (c'). Two scaling steps (d) and two scaling δ functions (e) in a box together with their associated four-vertex dressed linear quantum graphs (d') and (e'), respectively

We apply the Dirichlet boundary conditions at the open ends. In this case, spectral equation (3.6) becomes

$$\cos\left[k(S^0_{21}+S^0_{23})-\pi\gamma_0\right] = \\ = -|r|\cos\left[k(S^0_{21}-S^0_{23})\right], \quad (5.4)$$

where

$$\gamma_0 = 1 - \frac{1}{\pi}\arcsin\left(\frac{2}{\sqrt{4+(\lambda^0_2)^2}}\right) \quad (5.5)$$

and the reflection coefficient r is given by

$$r = \frac{\lambda^0_2}{2i-\lambda^0_2}. \quad (5.6)$$

Because $|r|<1$, the characteristic function of (5.4) also satisfies regularity condition (3.8). Therefore, the scaling δ function in a box is another example of a regular quantum graph.

Example 3: Combined scaling step and scaling δ-potential in a box (Fig. 4c). This is equivalent to a three-vertex dressed linear graph (Fig. 4c') with $\lambda_2 = \lambda^0_2 k > 0$. Spectral equation (3.6) then becomes

$$\cos\left[k(S^0_{21}+S^0_{23})-\pi\gamma_0\right] = \\ = a_1\cos\left[k(S^0_{21}-S^0_{23})-\pi\gamma_1\right], \quad (5.7)$$

where

$$\gamma_0 = 1 - \frac{1}{\pi}\arcsin\left(\frac{\beta_{12}+\beta_{23}}{\sqrt{(\beta_{12}+\beta_{23})^2+(\lambda^0_2)^2}}\right), \\ \gamma_1 = 1 - \frac{1}{\pi}\arcsin\left(\frac{\beta_{12}-\beta_{23}}{\sqrt{(\beta_{12}-\beta_{23})^2+(\lambda^0_2)^2}}\right), \quad (5.8)$$

and the coefficient a_1 is

$$a_1 = \sqrt{\frac{(\beta_{21}-\beta_{23})^2+(\lambda^0_2)^2}{(\beta_{21}+\beta_{23})^2+(\lambda^0_2)^2}} < 1. \quad (5.9)$$

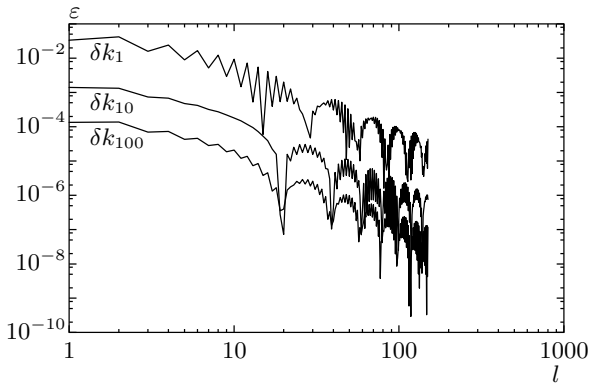

Fig. 5. Comparison between the exact eigenvalues k_n and the k_n values computed via (4.3) for the scaling step potential in Fig. 1. Shown is the relative error $\epsilon_n^{(l)} = |k_n^{(l)} - k_n|/k_n$, $n = 1, 10, 100$, of the result $k_n^{(l)}$ predicted by (4.3) compared to the numerically obtained exact result k_n as a function of the binary code length l of the orbits used in expansion (4.3). We used $b = 0.3$ and $\lambda = 1/2$

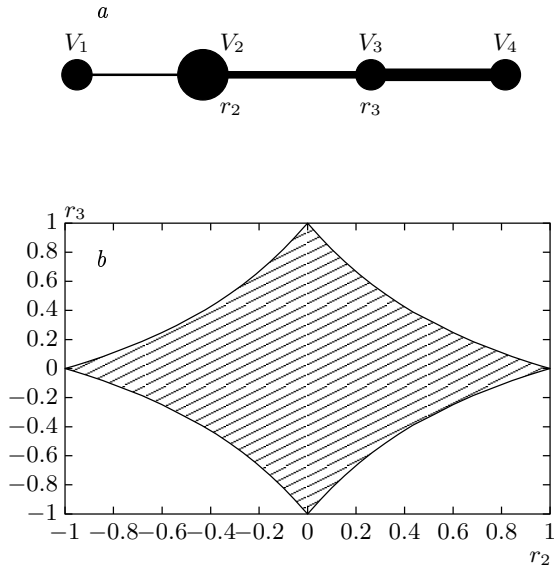

Fig. 6. Four-vertex linear chain graph (a) and the corresponding space (r_2, r_3) of reflection coefficients (b). The shaded region in the (r_2, r_3) space corresponds to the regular regime of the quantum graph shown in (a). This demonstrates that the subset of regular quantum graphs within the set of all four-vertex linear quantum graphs is non-empty and has a finite measure

Therefore, the characteristic function of (5.7) once again satisfies the regularity condition for any linear three-vertex graph with nontrivial bond potentials $(\beta_{21}^2 + \beta_{23}^2 \neq 0)$ [6].

Quantum graphs that are regular for all of their parameter values are quite exceptional. In general, quantum graphs may have a regular regime for a certain range of the parameter values or the regular regime may not exist at all. The following example illustrates this point.

Example 4: Two scaling steps in a box (Fig. 4d). As an example of a graph that has both a regular and an irregular regime, we consider a quantum particle in a box with two scaling steps (Fig. 4d), which is equivalent to the four-vertex linear graph shown in Fig. 4d'. Because there are no δ functions present, we have $\lambda_2 = \lambda_3 = 0$. We assume the Dirichlet boundary conditions at the dead ends of this graph. In this case, spectral equation (3.6) is given by

$$\sin(S_0 k) = -r_2 \sin(kS_1) - \\ - r_2 r_3 \sin(kS_2) + r_3 \sin(kS_3), \quad (5.10)$$

where

$$S_0 = S_{21}^0 + S_{23}^0 + S_{34}^0, \quad S_1 = S_{23}^0 + S_{34}^0 - S_{21}^0, \\ S_2 = S_{21}^0 + S_{34}^0 - S_{23}^0, \quad S_3 = S_{21}^0 + S_{23}^0 - S_{34}^0, \quad (5.11)$$

and

$$r_2 = \frac{\beta_{12} - \beta_{23}}{\beta_{12} + \beta_{23}}, \quad r_3 = \frac{\beta_{23} - \beta_{34}}{\beta_{23} + \beta_{34}} \quad (5.12)$$

are the reflection coefficients at the corresponding vertices V_i. For

$$|r_3| + |r_2 r_3| + |r_2| < 1, \quad (5.13)$$

the four-vertex linear graph (Figs. 4d' and 6a) is regular. Regularity condition (5.13) is fulfilled in a diamond-shaped region of the (r_2, r_3) parameter space shown as the shaded area in Fig. 6b. The difference between the regular and the irregular regimes is clearly reflected in the staircase functions. Figure 7a shows the staircase function $N(k)$ together with the average staircase $\bar{N}(k)$ in the regular regime for the parameter combination $r_2 = 0.2$ and $r_3 = 0.3$. The piercing-average condition is clearly satisfied. Figure 7b shows the staircase function $N(k)$ together with the average staircase $\bar{N}(k)$ in the irregular regime for the parameter combination $r_2 = 0.98$ and $r_3 = 0.99$. In this case, the piercing-average condition is clearly violated, consistently with the irregular nature of this regime.

Example 5: Two scaling δ functions in a box (Fig. 4e). This potential is equivalent to the four-vertex graph shown in Fig. 4e' with

$$\lambda_2 = \lambda_2^0 k > 0, \quad \lambda_3 = \lambda_3^0 k > 0,$$

and the Dirichlet boundary conditions at the dead ends

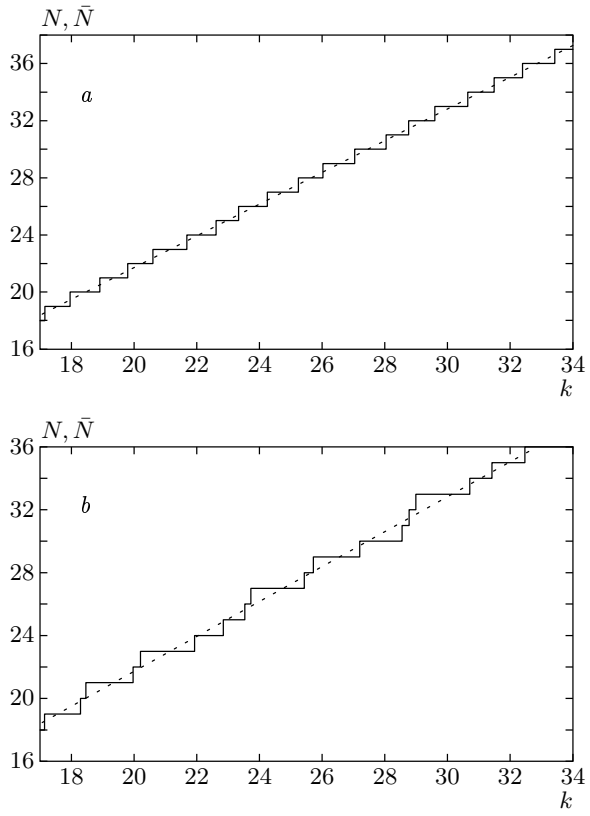

Fig. 7. The exact spectral staircase function $N(k)$ and its average $\bar{N}(k)$ for the regular $r_2 = 0.2$, $r_3 = 0.3$ (a) and the irregular $r_2 = 0.98$, $r_3 = 0.99$ (b) regimes of the four-vertex linear graph shown in Fig. 6a. In the regular regime (a), the average staircase function $\bar{N}(k)$ pierces every step of $N(k)$. This is not the case in (b), characteristic of the irregular regime

V_1 and V_4. In this case, spectral equation (3.6) is given by

$$\cos(kS_0 - \pi\gamma_0) = a_1 \cos(kS_1 - \pi\gamma_1) + \\ + a_2 \cos(kS_2 - \pi\gamma_2) + a_3 \cos(kS_3 - \pi\gamma_3), \quad (5.14)$$

where

$$a_1 = \frac{\lambda_2^0}{\sqrt{4 + (\lambda_2^0)^2}}, \quad a_2 = \frac{\lambda_3^0}{\sqrt{4 + (\lambda_3^0)^2}}, \\ a_3 = \frac{\lambda_2^0 \lambda_3^0}{\sqrt{[4 + (\lambda_2^0)^2][4 + (\lambda_3^0)^2]}} \quad (5.15)$$

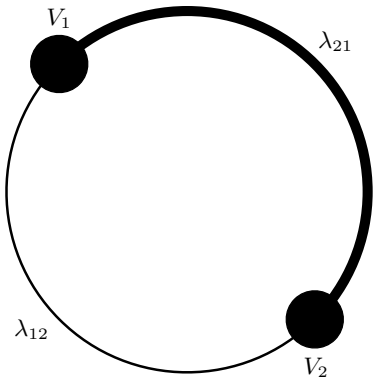

Fig. 8. Two-vertex circular graph. In the mathematically positive sense, β_{12} is the scaling coefficient of the bond connecting the vertex V_1 with the vertex V_2, β_{21} is the scaling coefficient of the bond connecting V_2 with V_1. This labelling is possible only in the absence of a magnetic field ($A_{ij} = 0$), where the sense of traversal of a bond is irrelevant

and

$$\gamma_0 = \frac{1}{\pi} \arcsin\left(\frac{\lambda_2^0 \lambda_3^0 - 4}{\sqrt{[4 + (\lambda_2^0)^2][4 + (\lambda_3^0)^2]}}\right), \\ \gamma_1 = \frac{1}{\pi} \arcsin a_2, \\ \gamma_2 = \frac{1}{\pi} \arcsin a_1, \\ \gamma_3 = \frac{1}{2}. \quad (5.16)$$

The sum of the amplitudes in (5.15) ranges between 0 and 3, and therefore, this system has regular and irregular regimes. The regular regime corresponds to a finite area in the $(\lambda_2^0, \lambda_3^0)$ parameter space. All linear chain graphs with a finite number of vertices and the Dirichlet boundary conditions at the two dead-end vertices at the beginning and at the end of the graph have a finite-measure regular regime and an irregular regime. This fact is proved in [10].

Graphs of a new type are marginal quantum graphs. A marginal quantum graph is defined by

$$\sum_{i=1}^{N_\Gamma} |a_i| = 1. \quad (5.17)$$

For marginal quantum graphs, apart from a small set of «special» graphs, explicit spectral formulas still exist. Explicit examples are provided by circular graphs (see Example 6) and star graphs (see Example 7).

Example 6: Scaling step potential in a box with periodic boundary conditions. This system is identical

with the two-vertex circular graph shown in Fig. 8. In the case of a circular graph, a minor notational problem arises because starting from a vertex V_1, e.g., the vertex V_2 can be directly reached via two different bonds. For the purposes of this example, we solve the problem as follows. We first introduce a positive sense of rotation, i.e., mathematically positive, or counterclockwise, for the circular graph in Fig. 8. We then introduce the scaling coefficient β_{12} referring to the bond that connects the vertex V_1 with the vertex V_2 traversing the graph in the mathematically positive sense. We introduce the scaling coefficient β_{21} that refers to the bond connecting V_2 with V_1, again in the mathematically positive sense. We use the same notation for the two reduced actions S^0_{12} and S^0_{21} referring to the two different bonds (in the mathematically positive sense), respectively. This notation is not confusing here, because no magnetic field is switched on ($A_{ij} = 0$). With this notation, the spectral equation is given by

$$\cos(kS_0) = a_1 + a_2\,\cos(kS_2), \tag{5.18}$$

where

$$S_0 = S^0_{12} + S^0_{21}, \quad S_1 = S^0_{12} + S^0_{21},$$

$$a_1 = \frac{4\beta_{12}\beta_{21}}{(\beta_{12}+\beta_{21})^2} \tag{5.19}$$

and

$$a_2 = \left(\frac{\beta_{12}-\beta_{21}}{\beta_{12}+\beta_{21}}\right)^2. \tag{5.20}$$

We note that $a_1 + a_2 = 1$. Condition (5.17) is satisfied and the circular quantum graph with a scaling step potential is marginal.

Although the strict inequality in Eq. (3.8) is violated, it is important to note that even in the marginal case, the separating points $\hat{k}_n$ are still not solutions to (5.18) in general. This occurs only for special parameter combinations, and therefore for special quantum graphs for which the equation

$$(-1)^{n+\mu+1} = a_1 + a_2\cos(\hat{k}_n S_2) \tag{5.21}$$

is exactly satisfied for some n. Because the sequence $\hat{k}_n$ is countable and Eq. (5.21) involves irrational frequency ratios and irrational coefficients in general, this equation is only accidentally satisfied for some n for a measure zero set of graph parameters. Hence, in general, even for marginal quantum graphs, the points $\hat{k}_n$ still serve as separating points and the roots of the spectral equation can still be obtained via expansion (4.3).

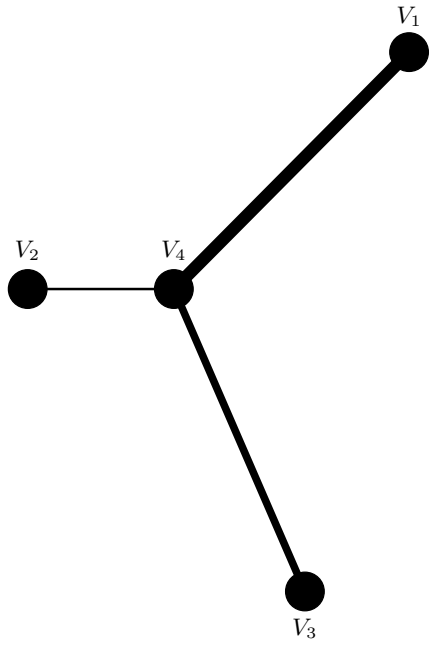

Fig. 9. Scaling star graph with three bonds and four vertices

Example 7: Star graph. Another example of a marginal quantum graph is provided by the star graph shown in Fig. 9. We consider the case with three different scaling potentials on its three bonds and the Dirichlet boundary conditions at the three dead ends. The spectral equation is given by

$$\cos(S_0 k) = a_1\cos(S_1 k) + \\ + a_2\cos(S_2 k) + a_3\cos(S_3 k), \tag{5.22}$$

where

$$\begin{aligned} S_0 &= S^0_{14}+S^0_{24}+S^0_{34}, \quad S_1 = S^0_{14}-S^0_{24}+S^0_{34}, \\ S_2 &= S^0_{14}-S^0_{24}-S^0_{34}, \quad S_3 = S^0_{14}+S^0_{24}-S^0_{34}, \end{aligned} \tag{5.23}$$

and

$$\begin{aligned} a_1 &= \frac{\beta_{14}-\beta_{24}+\beta_{34}}{\beta_{14}+\beta_{24}+\beta_{34}}, \\ a_2 &= \frac{-\beta_{14}+\beta_{24}+\beta_{34}}{\beta_{14}+\beta_{24}+\beta_{34}}, \\ a_3 &= \frac{\beta_{14}+\beta_{24}-\beta_{34}}{\beta_{14}+\beta_{24}+\beta_{34}}. \end{aligned} \tag{5.24}$$

It is straightforward to verify that

$$\sum_{i=1}^{3} |a_i| = 1$$

independently of the sign of each a_i in (5.24). Condition (5.17) is therefore satisfied and the star graph

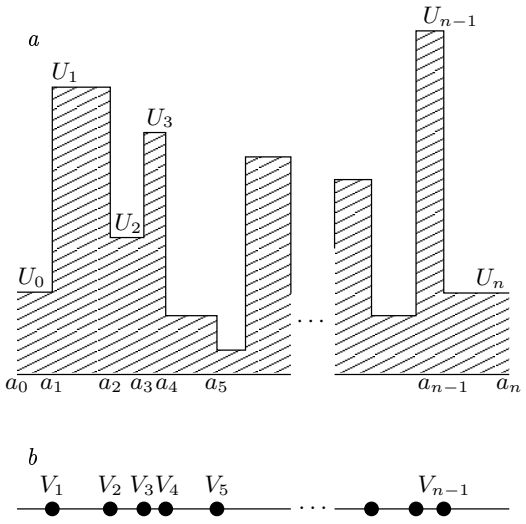

Fig. 10. Sketch of a piecewise constant potential («Manhattan potential») (*a*) and its associated linear graph (*b*)

shown in Fig. 9 is another example of a marginal quantum graph. As discussed in the context of Example 6, with the exception of a set of measure zero of the star-graph parameter space, spectral expansion (4.3) is still valid and can be used to obtain each of the star-graph eigenvalues individually, and independently of all the other eigenvalues.

6. SUMMARY, DISCUSSION, AND CONCLUSIONS

Exact periodic orbit expansions for the global density of states are known for many chaotic systems [15, 32, 33]. However, Eq. (4.3) is the first example of an explicit expression for the individual quantum-mechanical levels obtained as a function of the level index n for a classically chaotic system. Additional explicit quantization formulas may be found for other quantum graph systems, or even for quantum systems unrelated to quantum graphs as long as two essential requirements are fulfilled. First, an exact periodic orbit expansion for the density of states must exist. Second, it must be determined that one of the system levels, k_*, is the only one in an interval $\hat{k}'_* < k_* < \hat{k}''_*$. Then one can always obtain the corresponding periodic orbit expansion for k_*,

$$k_* = \int_{\hat{k}'_*}^{\hat{k}''_*} k\rho(k)dk, \tag{6.1}$$

based on the periodic orbit expansion for $\rho(k)$.

It is reasonable to expect that generically there exist separating points $\hat{k}'_*$ and $\hat{k}''_*$ that separate every k_* from its neighbors, such that k_* is the only root of the spectral equation in the interval $[\hat{k}'_*, \hat{k}''_*]$. Hence, expansions similar to (4.3) do exist in general. However, knowing the positions of the separators k'_* and k''_* around a particular level k_* does not help finding the separators for the other levels. The most important task in obtaining a general expression for all the levels of a quantum chaotic system is therefore to find a global function for the separating points similar to (3.10), which naturally enumerates the separators. Therefore, even though it might be possible to find the separators for a particular quantum level k_* for some systems and then to obtain a periodic orbit expansion for this level in accordance with (6.1), the expansion would work only for the level k_* and would not represent a formula that can be used to obtain other levels.

The problem of finding a global expression for the separating points as a function of their ordering index n is directly related to another well-known problem of spectral theory of differential operators, namely the problem of approximating staircase function (2.17) by a smooth average $\bar{N}(k)$. Indeed, suppose that there exists a separating point $\hat{k}'_n$, i.e., a solution of the equation

$$\bar{N}(\hat{k}') = N(k), \tag{6.2}$$

between every two roots of the spectral equation (similar to (3.20) and (3.21)). Because $\bar{N}(k)$ is a monotonic function, the separating points can then be found by inverting Eq. (6.2),

$$\hat{k}_N = k(N), \tag{6.3}$$

where the value of the staircase function plays the role of the separator index $\hat{k}_N$. Equation (6.3) generalizes Eq. (3.10), which can be used in (6.1) to obtain the periodic orbit expansions for all the roots.

The smooth curve defined by (6.3) with N considered a continuous variable intersects every stair of spectral staircase function (2.17). Unfortunately, finding a smooth function that approximates the spectral staircase function for a general differential operator with generic boundary conditions is a rather complicated task. It was proven by Weyl in 1912 that one can approximate $\bar{N}(k)$ by the phase-space volume of the system in question,

$$\bar{N}(E) \approx \int \Theta(E - H(x,p)) \frac{d^D x d^D p}{(2\pi\hbar)^D}, \tag{6.4}$$

where D is the dimensionality of the phase space, however this average is certainly not guaranteed to satisfy the «piercing average» condition (6.2). Since Weyl, this problem has been addressed by numerous researchers (see, e.g., [34]), who succeeded in giving many improved estimates for $\bar{N}(k)$ but none of them a priori satisfy (6.2).

The important feature of the regular quantum graph systems is that there exists a global piercing average (3.10), which uniformly enumerates all the points separating one root from another, and it is therefore possible to obtain formula (4.3) as a function of the index n. In other words, the index n in (4.3) is a quantum number, and expression (4.3) for the energy levels of a chaotic system in terms of classical periodic orbits can therefore be considered as a nonintegrable analogue of the EBK quantization scheme [11, 12].

It should be mentioned that despite the existence of a quantum number n in (4.3), the actual dependence of the energy levels on the value of its quantum number is quite different from the simple EBK scheme for integrable systems. The expansion of the fluctuating part of roots (3.11) involves an intricate, conditionally convergent series and is rather «chaotic». The difference in complexity of formulas (4.3) and the EBK formula apparently reflects the complexity of the geometry of the periodic orbits of the classically chaotic quantum graphs.

Y. D. and R. B. gratefully acknowledge financial support by NSF grants PHY-9900730 and PHY-9984075; Y. D. and R. V. J. by NSF grant PHY-9900746.

APPENDIX

For completeness, we here present a simple derivation of the spectral determinant in Eq. (2.8), starting from the boundary conditions at the vertex V_i,

$$\psi_{ij}(x)|_{x=0} = \varphi_i C_{ij} \tag{A.1}$$

and

$$\sum_{j=1}^{N_V} C_{ij} \left(i\frac{d}{dx_{ij}} + A_{ij} \right) \psi_{ij}(x_{ij})|_{x=0} = \lambda_i \varphi_i. \tag{A.2}$$

We represent the wave function

$$\psi_{ij}(x) = \\ = \frac{1}{\sqrt{\beta_{ij}k}} \left(a_{ij} \exp(-i\beta_{ij}kx) + b_{ij} \exp(i\beta_{ij}kx) \right) \tag{A.3}$$

that satisfies these boundary conditions as a superposition of the partial waves

$$\psi^{(i)}_{jj'}(x_j) = \delta_{jj'} \frac{\exp(i\,(-\beta_{ij}k + A_{ij})\,x_j)}{\sqrt{\beta_{ij}k}} + \\ + \sigma_{ji,ij'} \frac{\exp(i\,(\beta_{ij}k + A_{ij})\,x_j)}{\sqrt{\beta_{ij}k}} \tag{A.4}$$

scattering on the vertices of the graph. We thus have

$$\psi_{ij}(x_j) = \sum_{j'=1}^{N_V} a_{ij'} \psi^{(i)}_{j,j'}(x_j) = \\ = \frac{a_{ij}}{\sqrt{\beta_{ij}k}} \exp(-i\,(\beta_{ij}k - A_{i,j})\,x_j) + \\ + \frac{\exp(i\,(\beta_{ij}k + A_{i,j})\,x_j)}{\sqrt{\beta_{ij}k}} \sum_{j'=1}^{N_V} a_{ij'}\sigma_{ji,ij'}, \tag{A.5}$$

with the appropriate weights $a_{ij'}$ corresponding to the incoming flux on the bond $B_{j'i}$ towards the vertex V_i. Comparing this expression with (A.3) yields

$$b_{ij} = \sum_{j'=1}^{N_V} \sigma_{ji,ij'} a_{ij'}. \tag{A.6}$$

Substituting (A.5) into boundary conditions (A.1) and (A.2) at the vertex V_i, we obtain the respective relations

$$\sum_{j'=1}^{N_V} \frac{a_{ij'}}{\sqrt{\beta_{ij}k}} \left(\delta_{jj'} + \sigma_{ji,ij'} \right) = \varphi_i C_{ij} \tag{A.7}$$

and

$$\sum_{j,j'=1}^{N_V} C_{ij} a_{ij'} \sqrt{\beta_{ij}k} \left(\delta_{jj'} - \sigma_{ji,ij'} \right) = i\lambda_i \varphi_i. \tag{A.8}$$

Inserting (A.7) in (A.8), we obtain

$$C_{ij} \sum_{l,j'=1}^{N_V} C_{il} a_{ij'} \sqrt{\beta_{il}k} \left(\delta_{lj'} - \sigma^{(i)}_{l,j'} \right) = \\ = i\lambda_i \sum_{j'=1}^{N_V} \frac{a_{ij'}}{\sqrt{\beta_{ij}k}} \left(\delta_{jj'} + \sigma_{ji,ij'} \right). \tag{A.9}$$

In the case of the linear scaling $\lambda_i = k\lambda_i^0$, this yields

$$\sum_{j'=1}^{N_V} a_{ij'} C_{ij} \sum_{l=1}^{N_V} C_{il} \sqrt{\beta_{il}} \left(\delta_{lj'} - \sigma_{li,ij'} \right) = \\ = i\lambda_i^0 \sum_{j'=1}^{N_V} \frac{a_{ij'}}{\sqrt{\beta_{ij}}} \left(\delta_{jj'} + \sigma_{ji,ij'} \right). \tag{A.10}$$

Comparing the coefficients in front of $a_{ij'}$, we obtain

$$C_{ij}\sum_{l=1}^{N_V} C_{il}\delta_{lj'}\sqrt{\beta_{il}} - C_{ij}\sum_{l=1}^{N_V} C_{il}\sqrt{\beta_{il}}\sigma^{(i)}_{l,j'} - \\ - i\lambda_i^0\frac{\delta_{jj'}}{\sqrt{\beta_{ij}}} = \frac{i\lambda_i^0}{\sqrt{\beta_{ij}}}\sigma_{ji,ij'}, \quad \text{(A.11)}$$

or after performing the summation over l,

$$C_{ij}C_{ij'}\sqrt{\beta_{ij'}} - C_{ij}\Gamma^i_{i,j'} - \\ - i\lambda_i^0\frac{\delta_{jj'}}{\sqrt{\beta_{ij}}} = \frac{i\lambda_i^0}{\sqrt{\beta_{ij}}}\sigma_{ji,ij'}, \quad \text{(A.12)}$$

where

$$\Gamma^i_{i,j'} = \sum_{l=1}^{N_V} C_{il}\sqrt{\beta_{il}}\sigma_{li,ij'}.$$

Multiplying both sides by $C_{ij}\beta_{ij}$ and summing over j yields

$$v_i C_{ij'}\sqrt{\beta_{ij'}} - v_i\Gamma^i_{i,j'} - i\lambda_i^0 C_{ij'}\sqrt{\beta_{ij'}} = \\ = i\lambda_i^0\Gamma^i_{i,j'}, \quad \text{(A.13)}$$

where

$$v_i = \sum_j C_{ij}\beta_{ij}.$$

Hence,

$$\frac{v_i - i\lambda_i^0}{v_i + i\lambda_i^0}C_{ij'}\sqrt{\beta_{ij'}} = \Gamma^i_{i,j'}, \quad \text{(A.14)}$$

which can be used in (A.12) to obtain

$$C_{ij}C_{ij'}\sqrt{\beta_{ij'}} - C_{ij}\frac{v_i - i\lambda_i^0}{v_i + i\lambda_i^0}C_{ij'}\sqrt{\beta_{ij'}} - i\lambda_i^0\frac{\delta_{jj'}}{\sqrt{\beta_{ij}}} = \\ = \frac{i\lambda_i^0}{\sqrt{\beta_{ij}}}\sigma_{ji,ij'} \quad \text{(A.15)}$$

or

$$\sigma_{ji,ij'} = \left(-\delta_{jj'} + \frac{2\sqrt{\beta_{ij}\beta_{ij'}}}{v_i + i\lambda_i^0}\right)C_{ji}C_{ij'}. \quad \text{(A.16)}$$

We see that in the scaling case, the matrix elements $\sigma_{ji,ij'}$ of the vertex scattering matrix σ are k-independent constants.

The matrix element $\sigma_{ji,ij}$ has the meaning of the reflection coefficient from the vertex V_i along the bond B_{ij} and the elements $\sigma_{ji,ij'}$, $j \neq j'$ are the transmission coefficients for transitions between different bonds. Equation (A.6) can be written as

$$\mathbf{b} = \tilde{T}\mathbf{a}, \quad \text{(A.17)}$$

where

$$\tilde{T} \equiv \tilde{T}_{ij,nm} = \delta_{in}C_{ji}C_{nm}\sigma_{ji,im}. \quad \text{(A.18)}$$

In the symmetric basis $\psi_{ji}(L_{ij} - x) = \psi_{ij}(x)$, we have

$$\psi_{ji}(L_{ij}-x) = a_{ji}\frac{\exp\left[\left(i\left(-\beta_{ij}k+A_{ji}\right)\left(L_{ij}-x\right)\right]\right.}{\sqrt{\beta_{ij}k}} + \\ + b_{ji}\frac{\exp\left[i\left(\beta_{ij}k + A_{ji}\right)\left(L_{ij} - x\right)\right]}{\sqrt{\beta_{ij}k}} = \psi_{ij}(x), \quad \text{(A.19)}$$

and the coefficients a_{ij} and b_{ij} are therefore related as

$$\begin{aligned} a_{ji} &= b_{ij}\exp\left[i\left(\beta_{ij}k + A_{ij}\right)L_{ij}\right], \\ b_{ji} &= a_{ij}\exp\left[i\left(-\beta_{ij}k + A_{ij}\right)L_{ij}\right]. \end{aligned} \quad \text{(A.20)}$$

The coefficients a_{ij} and a_{ji} (b_{ij} and b_{ji}) are considered to be different, and the bonds of the graph are therefore «directed».

Equations (A.20) can be written in the matrix form

$$\mathbf{a} = P\tilde{D}(k)\mathbf{b}, \quad \text{(A.21)}$$

where $\mathbf{a}$ and $\mathbf{b}$ are $2N_B$-dimensional vectors of coefficients and $\tilde{D}$ is a diagonal matrix in the $2N_B \times 2N_B$ space of directed bonds,

$$\tilde{D}_{ij,pq}(k) = \delta_{ip}\delta_{jq}\exp\left[i\left(\beta_{ij}k + A_{ij}\right)L_{ij}\right], \quad \text{(A.22)}$$

and

$$P = \begin{pmatrix} 0 & 1_{N_B} \\ 1_{N_B} & 0 \end{pmatrix}, \quad \text{(A.23)}$$

where 1_{N_B} is the N_B-dimensional unit matrix. The pairs of indices (ij), (pq) identifying the bonds of the graph Γ play the role of the indices of the matrix $\tilde{D}(k)$.

Equations (A.21) and (A.17) together result in

$$\mathbf{a} = S(k)\mathbf{a}, \quad \text{(A.24)}$$

with the matrix $S(k)$ (the total graph scattering matrix) given by

$$S(k) = D(k)T, \quad \text{(A.25)}$$

where $D = P\tilde{D}P$ and $T = P\tilde{T}$.

REFERENCES

1. L. D. Landau and E. M. Lifshitz, *Quantum Mechanics*, Pergamon Press, Oxford, New York (1977).
2. A. Messiah, *Quantum Mechanics*, North-Holland, Amsterdam (1961).

3. S. Flügge, *Practical Quantum Mechanics*, Springer, Berlin (1999).

4. R. Blümel, Yu. Dabaghian, and R. V. Jensen, submitted to Phys. Rev. Lett.

5. Yu. Dabaghian, R. V. Jensen, and R. Blümel, Pis'ma v ZhETF **74**, 258 (2001).

6. R. Blümel, Yu. Dabaghian, and R. V. Jensen, submitted to Phys. Rev. E.

7. H. Bohr, *Almost Periodic Functions*, Chelsea Publishing, New York (1951).

8. H. Friedrich, *Theoretical Atomic Physics*, Springer, Berlin (1990).

9. H.-J. Stöckmann, *Quantum Chaos*, Cambridge University Press, Cambridge (1999).

10. R. Blümel, Yu. Dabaghian, and R. V. Jensen, *Mathematical Foundations of Regular Quantum Graphs*, in preparation.

11. M. Gutzwiller, *Chaos in Classical and Quantum Mechanics*, Springer, New York (1990).

12. J. B. Keller, Ann. Phys. (N.Y.) **4**, 180 (1958).

13. R. I. Szabo, LANL archive hep-th/9608068.

14. M. V. Berry, in *New Trends in Nuclear Collective Dynamics*, Springer Proc. in Physics, ed. by Y. Abe, H. Huriuchi, and K. Matsuyanagi, Springer Verlag, Berlin (1991), Vol. 58, p. 177.

15. J.-P. Roth, in *Lecture Notes in Mathematics: Théorie du Potentiel*, ed. by A. Dold and B. Eckmann, Springer, Berlin (1984), Vol. 1096, p. 521.

16. T. Kottos and U. Smilansky, Phys. Rev. Lett. **79**, 4794 (1997); Ann. Phys. (N.Y.) **274**, 76 (1999).

17. M. Pascaud and G. Montambaux, Phys. Rev. Lett. **82**, 4512 (1999).

18. H. Schanz and U. Smilansky, Phys. Rev. Lett. **84**, 1427 (2000).

19. Y. Dabaghian, R. V. Jensen, and R. Blümel, Phys. Rev. E **63**, 066201 (2001).

20. Y. C. Lai, C. Grebogi, R. Blümel, and M. Ding, Phys. Rev. A **45**, 8284 (1992).

21. M. Keeler and T. J. Morgan, Phys. Rev. Lett. **80**, 5726 (1998).

22. V. I. Arnold and A. Avez, *Ergodic Problems of Classical Mechanics*, Addison Wesley, Redwood City (1989).

23. V. I. Arnold, *Mathematical Methods of Classical Mechanics*, Springer, New York (1997).

24. E. Akkermans, A. Comtet, J. Desbois, G. Montambaux, and C. Texier, LANL archive cond-mat/9911183.

25. F. Barra and P. Gaspard, Phys. Rev. E **63**, 066215 (2001).

26. R. E. Prange, E. Ott, T. M. Antonsen, B. Georgeot, and R. Blümel, Phys. Rev. E **53**, 207 (1996).

27. R. Blümel, T. M. Antonsen, Jr., B. Georgeot, E. Ott, and R. E. Prange, Phys. Rev. Lett. **76**, 2476 (1996); Phys. Rev. E **53**, 3284 (1996).

28. L. Sirko, P. M. Koch, and R. Blümel, Phys. Rev. Lett. **78**, 2940 (1997).

29. U. Smilansky, in *Chaos et Physique Quantique–Chaos and Quantum Physics, Les Houches session LII* (1989), ed. by M.-J. Giannoni, A. Voros, and J. Zinn-Justin, Elsevier Science Publishers, Amsterdam (1991), p. 371.

30. R. Courant and D. Hilbert, *Methods of Mathematical Physics*, Interscience Publishers, New York (1953).

31. R. Blümel and Yu. Dabaghian, submitted to J. Math. Phys.

32. A. Selberg, J. Indian Math. Soc. B **20**, 47 (1956); reprinted in *Atle Selberg: Collected Works*, Springer, Berlin (1989), Vol. 1, p. 423.

33. K. G. Anderson and R. B. Melrose, Inv. Math. **41**, 197 (1977).

34. H. P. Baltes and E. R. Hilf, *Spectra of Finite Systems*, Bibliographisches Institut AG, Zürich (1976).